JAN 31 1947

NATIONAL ADVISORY COMMITTEE FOR AERONAUTICS

TECHNICAL NOTE

No. 1156

COLUMN AND PLATE COMPRESSIVE STRENGTHS OF AIRCRAFT STRUCTURAL MATERIALS

EXTRUDED 0-1HTA MAGNESIUM ALLOY

By George J. Heimerl and Donald E. Niles

Langley Memorial Aeronautical Laboratory
Langley Field, Va.

Washington
January 1947

N A C A LIBRARY
LANGLEY MEMORIAL AERONAUTICAL
LABORATORY
Langley Field, Va.

NASA Technical Library
3 1176 01425 7696

NATIONAL ADVISORY COMMITTEE FOR AERONAUTICS

TECHNICAL NOTE NO. 1156

COLUMN AND PLATE COMPRESSIVE STRENGTHS OF AIRCRAFT STRUCTURAL MATERIALS

EXTRUDED O-1HTA MAGNESIUM ALLOY

By George J. Heimerl and Donald E. Niles

SUMMARY

Column and plate compressive strengths of extruded O-1HTA magnesium alloy were determined both within and beyond the elastic range from tests of flat-end H-section columns and from local-instability tests of H-, Z-, and channel-section columns. These tests are part of an extensive research investigation to provide data on the structural strength of various aircraft materials. The results are presented in the form of curves and charts that are suitable for use in the design and analysis of aircraft structures.

INTRODUCTION

Column and plate members that fail by instability are basic elements in an aircraft structure. For the design of structurally efficient aircraft, the strength of these elements must be known for the various aircraft materials. An extensive research program has therefore been undertaken at the Langley Memorial Aeronautical Laboratory to establish the column and plate compressive strengths of a number of the alloys available for use in aircraft structures. The alloys already investigated include 24S-T and 17S-T aluminum-alloy sheet and extruded 75S-T, 24S-T, R303-T, and 14S-T aluminum alloys (references 1 to 6, respectively).

Because information on high-strength magnesium alloys comparable with that now available for aluminum alloys is needed, extruded O-1HTA magnesium alloy has been included in the investigation. The results of the tests to determine the column and plate compressive strengths of extruded O-1HTA magnesium alloy are presented herein.

SYMBOLS

L	length of column
ρ	radius of gyration
c	fixity coefficient used in Euler column formula
$\frac{L}{\rho\sqrt{c}}$	effective slenderness ratio of column
b_F, t_F	width and thickness, respectively, of flange of H-, Z-, or channel section (see fig. 1)
b_W, t_W	width and thickness, respectively, of web of H-, Z-, or channel section (see fig. 1)
r	radius of corner fillet (see fig. 1)
k_W	nondimensional coefficient used with b_W and t_W in plate-buckling formula (see figs. 2 and 3 taken from reference 7)
E_c	modulus of elasticity in compression, taken as 6500 ksi for extruded O-1HTA magnesium alloy
τ	nondimensional coefficient (The value of τ is so determined that, when the effective modulus of elasticity τE_c is substituted for E_c in the equation for elastic buckling of columns, the computed critical stress agrees with the experimentally observed value. The coefficient τ is equal to unity within the elastic range and decreases with increasing stress beyond the elastic range.)
η	nondimensional coefficient for compressed plates corresponding to τ for columns
μ	Poisson's ratio, taken as 0.3 for extruded O-1HTA magnesium alloy
σ_{cr}	critical compressive stress
$\bar{\sigma}_{max}$	average compressive stress at maximum load
σ_{cy}	compressive yield stress

METHODS OF TESTING AND ANALYSIS

The specimens and methods of testing and analysis employed to determine the compressive stress-strain curves and the column and plate compressive strengths were similar to those described in reference 6 with the following exceptions:

In order to make the compressive stress-strain tests of single-thickness specimens, a modified Montgomery-Templin type of compression fixture (shown in fig. 4) utilizing grooved steel plates to support the specimens was used for most of the tests. The strains were measured by means of either one or two wire strain gages mounted at the middle of the faces of the specimen (see fig. 4) and were recorded together with the load by autographic load-strain equipment.

The nominal cross-sectional dimensions of all the flat-end columns used to determine the column strength were $b_F = 0.56$ inch, $b_W = 1.37$ inches, and $t_W = 0.125$ inch.

RESULTS AND DISCUSSION

Compressive Properties

The compressive stress-strain curves that apply to the extruded O-1HTA magnesium alloy used in this investigation are summarized in figure 5. The variation in compressive yield stress shown by the dashed curves indicates the maximum differences that were found to exist between the average values obtained at the ends of the different 20-foot extrusions; only a single curve is shown where the variation is small. The average value of σ_{cy} that applies to the entire cross section of the flat-end H-section columns is 34.1 ksi. The average values of σ_{cy} that apply to all the local-instability tests are 34.1 ksi for the flange material and 33.1 ksi for the web material.

The variation of compressive properties over a cross section of the largest extrusion is illustrated in figure 6. Each value of σ_{cy} represents the test results for a single-thickness compression specimen cut from the section at the position indicated. Values of σ_{cy} for the web are somewhat lower than those for the flange. Individual values for the web obtained from tests of the other extrusions, however, were in some instances as high or slightly higher than those obtained in some parts of the flanges.

Column and Plate Compressive Strengths

Because the compressive properties of an extruded magnesium alloy may vary, the data and charts of the present paper should not be used for design purposes for extrusions of O-1HTA magnesium alloy that have appreciably different compressive properties from those reported herein - unless a suitable method is devised for adjusting test results to account for variations in material properties. (Average values of σ_{cy} that apply are given in round numbers in figs. 7, 8, and 10 to 13.)

The results of the column and local-instability tests of extruded O-1HTA magnesium alloy are summarized herein; a discussion of basic relationships is given in reference 1.

Column strength.- The column curve of figure 7 shows the results of the flat-end H-section column tests. The fixity coefficient c was taken equal to 4 on the basis of test results for flat-end aluminum-alloy columns. The test points for three column tests $\left(\frac{L}{\rho\sqrt{c}}\right.$ of about 10$\left.\right)$ are not shown because these columns developed local instability after column buckling had occurred. Thus, the average compressive stress at maximum load $\bar{\sigma}_{max}$ (about 39.5 ksi for these three tests) would probably not represent the column strength if only column buckling had taken place. In these tests, however, visible column buckling was observed at a stress of about 34 ksi, and the short-dashed line shown in figure 7 (for values of $\frac{L}{\rho\sqrt{c}}$ from about 10 to 20) gives a conservative estimate of the column strength in this region. None of the other columns developed local instability.

The ratio of length to crookedness was greater than 1000 in all cases. (Crookedness is defined as the distance from a point at the midsection of a column from a straight line drawn between corresponding points at the end sections of the column.) Some effect of column curvature or imperfection, however, is indicated by the test values for $\frac{L}{\rho\sqrt{c}}$ of about 71 and 81 (see fig. 7) falling slightly below the Euler curve.

The reduction of the effective modulus of elasticity τE_c with increase in stress is indicated in figure 8 by the variation of τ with stress.

Plate compressive strength.- The results of the local-instability tests of the H-, Z-, and channel-section columns used

to determine the plate compressive strength are given in tables 1, 2, and 3, respectively. The instability of the plate elements of an H-section column under test is illustrated in figure 9.

The plate-buckling curves, analogous to the column curve of figure 7, are shown in figure 10. The reduction of the effective modulus of elasticity for plates ηE_c with increase in stress is indicated by the variation of η with stress, which is shown with the curve for τ in figure 8. The curves for both τ and η diverge from unity at a stress below that for which there is any visible divergence of the stress-strain curves from straight lines (see fig. 5) and indicate some effects of initial curvature or other column or plate imperfections.

The variation of the actual critical stress σ_{cr} with the theoretical critical stress σ_{cr}/η computed for elastic buckling by means of the formula and curves of figures 2 and 3 is shown in figure 11.

In order to illustrate the difference between the critical stress σ_{cr} and the average stress at maximum load $\bar{\sigma}_{max}$, the variation of σ_{cr} with $\sigma_{cr}/\bar{\sigma}_{max}$ is shown in figure 12. Because values of $\bar{\sigma}_{max}$ may be required in strength calculations, the variation of $\bar{\sigma}_{max}$ with σ_{cr}/η is shown in figure 13.

The data for H-sections describe slightly higher curves than those indicated for Z- and channel sections in figures 10 to 13. A reason for somewhat higher values of $\bar{\sigma}_{max}$ being obtained for H-sections than for Z- and channel sections for a given value of σ_{cr}/η (fig. 13) may be that the flange material tends to be somewhat stronger than the web material (see fig. 6) and forms a higher percentage of the total cross-sectional area for the H-section than for the Z- or channel sections. The results indicated by the individual curves obtained for the two classes of section are consistent with the comparable results for extruded aluminum alloys (references 3 to 5) for which the flange material was also stronger than the web material.

Langley Memorial Aeronautical Laboratory
National Advisory Committee for Aeronautics
Langley Field, Va., July 12, 1946

REFERENCES

1. Lundquist, Eugene E., Schuette, Evan H., Heimerl, George J., and Roy, J. Albert: Column and Plate Compressive Strengths of Aircraft Structural Materials. 24S-T Aluminum-Alloy Sheet. NACA ARR No. L5F01, 1945.

2. Heimerl, George J., and Roy, J. Albert: Column and Plate Compressive Strengths of Aircraft Structural Materials. 17S-T Aluminum-Alloy Sheet. NACA ARR No. L5F08, 1945.

3. Heimerl, George J., and Roy, J. Albert: Column and Plate Compressive Strengths of Aircraft Structural Materials. Extruded 75S-T Aluminum Alloy. NACA ARR No. L5F08a, 1945.

4. Heimerl, George J., and Roy, J. Albert: Column and Plate Compressive Strengths of Aircraft Structural Materials. Extruded 24S-T Aluminum Alloy. NACA ARR No. L5F08b, 1945.

5. Heimerl, George J., and Fay, Douglas P.: Column and Plate Compressive Strengths of Aircraft Structural Materials. Extruded R303-T Aluminum Alloy. NACA ARR No. L5H04, 1945.

6. Heimerl, George J., and Niles, Donald E.: Column and Plate Compressive Strengths of Aircraft Structural Materials. Extruded 14S-T Aluminum Alloy. NACA ARR No. L6D19, 1946.

7. Kroll, W. D., Fisher, Gordon P., and Heimerl, George J.: Charts for Calculation of the Critical Stress for local Instability of Columns with I-, Z-, Channel, and Rectangular-Tube Section. NACA ARR No. 3K04, 1943.

TABLE 1.- DIMENSIONS AND TEST RESULTS FOR H-SECTION

COLUMNS THAT DEVELOP LOCAL INSTABILITY

Column	t_W (in.)	t_F (in.)	b_W (in.)	b_F (in.)	L (in.)	$\frac{L}{b_W}$	$\frac{t_W}{t_F}$	$\frac{b_W}{t_W}$	$\frac{b_F}{b_W}$	k_W (fig. 2)	$\frac{b_W}{t_W}\sqrt{\frac{12(1-\mu^2)}{k_W}}$	$\frac{\sigma_{cr}}{\eta}$ (ksi) (a)	σ_{cr} (ksi)	$\bar{\sigma}_{max}$ (ksi)	$\frac{\sigma_{cr}}{\bar{\sigma}_{max}}$
1a	0.126	0.128	1.37	1.07	4.70	3.4	0.99	10.82	0.785	1.24	32.1	62.2	33.0	34.6	0.962
1b	.127	.128	1.37	1.07	4.83	3.6	.99	10.71	.790	1.22	32.1	62.4	33.9	34.4	.985
2a	.127	.128	1.37	1.10	5.17	3.8	.99	10.79	.804	1.18	32.8	59.8	31.9	34.6	.922
2b	.126	.128	1.37	1.08	5.16	3.8	.99	10.80	.790	1.22	32.3	61.5	32.6	34.5	.945
3a	.126	.128	1.37	1.14	5.50	4.0	.99	10.79	.842	1.10	34.0	55.5	32.9	34.6	.951
3b	.126	.128	1.37	1.14	5.50	4.0	.99	10.79	.842	1.10	34.0	55.5	31.9	34.3	.930
4	.124	.123	1.86	1.12	6.91	3.7	1.01	15.06	.602	1.93	35.8	50.0	32.9	33.3	.988
5a	.124	.123	1.86	1.21	8.21	4.4	1.01	15.06	.652	1.67	38.5	43.3	32.7	33.1	.988
5b	.124	.123	1.86	1.21	8.24	4.4	1.01	15.02	.650	1.67	38.4	43.6	32.8	33.2	.988
5c	.124	.123	1.86	1.21	8.22	4.4	1.01	15.08	.650	1.68	38.5	43.3	32.4	33.1	.979
6a	.123	.123	1.86	1.41	9.77	5.2	1.00	15.12	.756	1.29	43.9	33.3	29.0	30.2	.961
6b	.124	.123	1.86	1.41	9.77	5.2	1.01	15.06	.756	1.29	43.8	33.4	28.6	30.2	.947
6c	.124	.123	1.86	1.41	9.73	5.2	1.01	15.03	.756	1.29	43.8	33.4	28.0	29.9	.936
7a	.124	.124	1.86	1.55	11.24	6.0	1.00	15.11	.831	1.12	47.3	28.7	24.6	27.6	.893
7b	.124	.124	1.86	1.55	11.27	6.0	1.01	14.98	.832	1.10	47.3	28.7	24.2	27.4	.882
7c	.124	.124	1.86	1.55	11.22	6.0	1.00	15.04	.834	1.10	47.4	28.5	24.8	27.5	.903
8a	.122	.121	2.37	1.30	9.07	3.8	1.01	19.38	.548	2.24	42.8	35.0	29.5	30.2	.976
8b	.122	.121	2.37	1.30	9.12	3.9	1.01	19.33	.550	2.23	42.8	35.1	28.1	29.6	.949
8c	.123	.121	2.37	1.30	9.06	3.8	1.01	19.19	.551	2.22	42.6	35.4	28.9	29.9	.967
9a	.123	.122	2.37	1.54	11.91	5.0	1.01	19.20	.652	1.67	49.1	26.6	23.8	24.5	.971
9b	.123	.121	2.37	1.54	11.90	5.0	1.01	19.31	.650	1.67	49.4	26.3	24.0	25.0	.961
9c	.123	.122	2.37	1.54	11.87	5.0	1.00	19.29	.650	1.69	49.1	26.6	23.1	24.5	.943
10a	.123	.121	2.37	1.78	14.23	6.0	1.02	19.20	.753	1.28	56.1	20.4	18.8	23.2	.810
10b	.122	.122	2.37	1.78	14.21	6.0	1.00	19.35	.751	1.30	56.0	20.5	18.5	23.1	.801
11a	.123	.122	2.37	1.93	14.68	6.2	1.00	19.38	.812	1.15	59.8	17.9	15.7	22.7	.692
11b	.123	.122	2.37	1.93	14.70	6.2	1.00	19.27	.816	1.14	59.7	18.0	17.1	22.6	.757
11c	.123	.123	2.37	1.93	14.71	6.2	1.00	19.25	.816	1.14	59.6	18.1	16.6	22.8	.728
12a	.119	.122	3.00	1.35	11.95	4.0	.98	25.18	.449	3.15	46.9	29.2	25.8	27.6	.935
12b	.120	.122	3.00	1.35	12.00	4.0	.98	25.07	.448	3.15	46.7	29.4	25.4	27.1	.937
12c	.120	.122	3.00	1.35	12.00	4.0	.98	25.16	.448	3.15	46.9	29.2	25.0	27.4	.912
13a	.120	.122	3.00	1.65	14.67	4.9	.98	25.13	.549	2.32	54.5	21.6	19.6	24.2	.810
13b	.119	.122	3.00	1.65	14.66	4.9	.98	25.18	.548	2.32	54.6	21.5	19.4	24.1	.805
14a	.119	.122	3.00	1.95	16.79	5.6	.98	25.20	.648	1.76	62.8	16.3	15.7	22.4	.703
14b	.119	.122	3.00	1.95	16.77	5.6	.98	25.18	.648	1.76	62.8	16.3	16.1	22.6	.713
14c	.120	.122	3.00	1.95	16.79	5.6	.98	25.05	.648	1.74	62.8	16.2	16.0	22.5	.711
15a	.119	.122	3.00	2.44	18.56	6.2	.98	25.13	.814	1.18	76.6	10.9	11.2	21.2	.528
15b	.119	.122	3.00	2.44	18.57	6.2	.97	25.25	.814	1.18	76.8	10.9	10.5	21.0	.500
15c	.119	.123	3.00	2.44	18.57	6.2	.97	25.25	.814	1.19	76.7	10.9	11.1	21.0	.529

[a] $\frac{\sigma_{cr}}{\eta} = \frac{k_W \pi^2 E_c t_W^2}{12(1-\mu^2) b_W^2}$, where E_c = 6500 ksi and μ = 0.3.

NATIONAL ADVISORY
COMMITTEE FOR AERONAUTICS

TABLE 2.- DIMENSIONS AND TEST RESULTS FOR Z-SECTION

COLUMNS THAT DEVELOP LOCAL INSTABILITY

Column	t_W (in.)	t_F (in.)	b_W (in.)	b_F (in.)	L (in.)	$\frac{L}{b_W}$	$\frac{t_W}{t_F}$	$\frac{b_W}{t_W}$	$\frac{b_F}{b_W}$	k_W (fig. 3)	$\frac{b_W}{t_W}\sqrt{\frac{12(1-\mu^2)}{k_W}}$	$\frac{\sigma_{cr}}{\eta}$ (ksi) (a)	σ_{cr} (ksi)	$\bar{\sigma}_{max}$ (ksi)	$\frac{\sigma_{cr}}{\bar{\sigma}_{max}}$
1a	0.127	0.128	1.37	1.03	4.84	3.5	0.99	10.83	0.751	1.53	28.9	76.6	32.5	35.3	0.921
1b	.127	.128	1.37	1.03	4.84	3.5	.99	10.81	.749	1.54	28.8	77.4	34.1	35.7	.955
2	.127	.128	1.37	1.15	5.50	4.0	.99	10.80	.838	1.26	31.8	63.5	33.6	34.6	.971
3a	.124	.123	1.87	1.09	6.94	3.7	1.01	15.06	.580	2.30	32.8	59.6	32.2	33.5	.961
3b	.124	.123	1.87	1.09	6.93	3.7	1.01	15.11	.580	2.30	32.9	59.2	33.2	33.7	.985
3c	.124	.124	1.87	1.09	6.94	3.7	1.01	15.09	.581	2.30	32.9	59.3	33.1	33.6	.985
4a	.124	.124	1.87	1.22	8.23	4.4	1.00	15.05	.650	1.92	36.9	49.8	31.4	33.5	.937
4b	.124	.124	1.87	1.22	8.23	4.4	1.00	15.07	.650	1.92	36.9	49.7	31.6	33.0	.958
4c	.124	.123	1.87	1.22	8.24	4.4	1.01	15.08	.649	1.92	36.0	49.6	32.4	33.4	.970
5a	.124	.124	1.87	1.41	9.73	5.2	1.00	15.08	.751	1.51	40.6	39.0	30.6	32.4	.944
5b	.124	.124	1.87	1.43	9.74	5.2	1.00	15.05	.762	1.48	40.9	38.3	30.5	32.1	.950
5c	.124	.124	1.87	1.43	9.75	5.2	1.01	15.07	.761	1.48	40.9	38.3	28.7	30.8	.932
6a	.124	.124	1.87	1.55	11.25	6.0	1.00	15.07	.829	1.27	44.2	32.9	27.3	28.7	.952
6b	.125	.124	1.87	1.56	11.25	6.0	1.00	15.04	.832	1.27	44.2	32.9	27.2	29.3	.928
6c	.125	.124	1.87	1.56	11.20	6.0	1.01	15.03	.832	1.26	44.2	32.8	27.5	29.1	.946
7	.123	.121	2.37	1.30	9.47	4.0	1.02	19.27	.547	2.50	40.3	39.6	30.0	31.6	.949
8a	.123	.121	2.37	1.54	11.86	5.0	1.02	19.28	.647	1.90	46.2	30.0	24.7	26.8	.922
8b	.123	.121	2.37	1.54	11.89	5.0	1.02	19.29	.646	1.90	46.2	30.0	24.9	26.1	.954
8c	.123	.121	2.37	1.54	11.89	5.0	1.02	19.31	.647	1.90	46.4	29.9	24.4	26.3	.928
9a	.123	.121	2.37	1.78	14.25	6.0	1.01	19.32	.749	1.51	52.0	23.7	20.9	24.1	.867
9b	.123	.122	2.37	1.78	14.24	6.0	1.01	19.29	.749	1.51	51.9	23.8	21.0	24.3	.864
9c	.123	.122	2.37	1.78	14.24	6.0	1.01	19.29	.749	1.51	52.0	23.8	21.0	24.3	.864
10a	.123	.123	2.37	1.93	14.68	6.2	1.00	19.32	.813	1.32	55.6	20.8	18.6	23.3	.798
10b	.123	.122	2.37	1.93	14.69	6.2	1.00	19.33	.815	1.31	55.8	20.6	16.9	23.2	.728
10c	.122	.122	2.37	1.93	14.58	6.1	1.00	19.36	.816	1.31	55.9	20.5	17.2	23.3	.738
11	.117	.121	3.00	1.33	14.60	4.9	.97	25.66	.442	3.47	45.5	31.0	26.1	28.2	.926
12a	.117	.121	3.00	1.34	11.85	4.0	.97	25.67	.448	3.44	45.8	30.6	24.3	27.1	.897
12b	.117	.121	3.00	1.35	11.98	4.0	.97	25.67	.450	3.43	45.8	30.6	25.5	27.5	.927
12c	.117	.121	3.00	1.35	11.98	4.0	.97	25.69	.451	3.43	45.9	30.5	25.6	27.5	.931
13	.117	.121	3.00	1.66	14.60	4.9	.97	25.69	.554	2.61	52.5	23.2	20.4	23.7	.861
14a	.117	.121	3.00	1.88	16.71	5.6	.96	25.65	.627	2.12	58.2	18.9	17.3	22.4	.772
14b	.117	.121	3.00	1.89	16.70	5.6	.97	25.63	.629	2.11	58.3	18.9	16.8	22.6	.743
14c	.117	.121	3.00	1.89	16.72	5.6	.97	25.65	.628	2.11	58.4	18.8	17.6	22.7	.775
15a	.117	.122	3.00	2.44	18.67	6.2	.96	25.65	.812	1.39	71.9	12.4	11.3	20.6	.549
15b	.117	.122	3.00	2.44	18.63	6.2	.96	25.64	.811	1.39	71.9	12.4	10.7	20.4	.524
15c	.117	.122	3.00	2.44	18.51	6.2	.96	25.62	.812	1.39	71.8	12.4	10.5	20.6	.510

[a] $\frac{\sigma_{cr}}{\eta} = \frac{k_W \pi^2 E_c t_W^2}{12(1-\mu^2) b_W^2}$, where E_c = 6500 ksi and μ = 0.3.

NATIONAL ADVISORY
COMMITTEE FOR AERONAUTICS

TABLE 3.- DIMENSIONS AND TEST RESULTS FOR CHANNEL-SECTION

COLUMNS THAT DEVELOP LOCAL INSTABILITY

Column	t_W (in.)	t_F (in.)	b_W (in.)	b_F (in.)	L (in.)	$\frac{L}{b_W}$	$\frac{t_W}{t_F}$	$\frac{b_W}{t_W}$	$\frac{b_F}{b_W}$	k_W (fig. 3)	$\frac{b_W}{t_W}\sqrt{\frac{12(1-\mu^2)}{k_W}}$	$\frac{\sigma_{cr}}{\eta}$ (ksi) (a)	σ_{cr} (ksi)	$\bar{\sigma}_{max}$ (ksi)	$\frac{\sigma_{cr}}{\bar{\sigma}_{max}}$
1a	0.127	0.128	1.37	1.02	5.15	3.8	1.00	10.71	0.744	1.54	28.5	78.9	33.5	33.9	0.988
1b	.129	.128	1.37	1.02	5.15	3.8	1.00	10.62	.747	1.53	28.4	79.6	33.5	34.1	.982
2a	.127	.127	1.37	1.08	5.17	3.8	1.00	10.78	.792	1.39	30.3	70.0	33.0	33.8	.976
2b	.127	.127	1.37	1.08	5.16	3.8	.99	10.81	.792	1.39	30.3	69.9	32.9	34.1	.965
3a	.123	.122	1.87	.997	6.95	3.7	1.01	15.18	.532	2.64	30.8	67.4	33.5	33.9	.988
3b	.124	.122	1.87	.996	6.95	3.7	1.01	15.16	.532	2.64	30.9	67.4	33.2	34.0	.976
3c	.123	.122	1.87	.995	6.95	3.7	1.01	15.17	.531	2.64	30.8	67.4	33.3	33.9	.982
4a	.123	.122	1.87	.997	8.25	4.4	1.01	15.18	.532	2.62	31.0	66.8	32.9	33.3	.988
4b	.123	.122	1.87	.997	8.23	4.4	1.01	15.19	.532	2.62	31.0	66.7	33.0	33.3	.991
5	.123	.122	1.87	1.02	9.75	5.2	1.01	15.18	.543	2.52	31.6	64.3	32.6	33.4	.976
6a	.124	.123	1.87	1.10	6.94	3.7	1.01	15.06	.589	2.18	33.7	56.5	32.8	33.5	.979
6b	.124	.123	1.87	1.11	6.94	3.7	1.01	15.06	.590	2.18	33.7	56.5	32.8	33.3	.985
7a	.125	.123	1.87	1.21	8.25	4.4	1.01	15.03	.644	1.92	35.8	50.0	32.6	32.9	.991
7b	.124	.123	1.87	1.21	8.25	4.4	1.01	15.14	.644	1.93	36.0	49.5	33.1	33.2	.997
7c	.124	.123	1.87	1.21	8.23	4.4	1.01	15.16	.644	1.94	36.0	49.5	32.9	33.0	.997
8a	.124	.123	1.87	1.40	9.75	5.2	1.01	15.09	.745	1.52	40.4	39.3	30.7	32.0	.959
8b	.124	.124	1.87	1.40	9.75	5.2	1.00	15.10	.745	1.53	40.3	39.5	30.9	32.3	.957
8c	.124	.124	1.87	1.40	9.76	5.2	1.00	15.09	.745	1.53	40.3	39.5	31.4	32.0	.981
9a	.122	.121	2.37	1.53	11.88	5.0	1.01	19.42	.644	1.94	46.1	30.2	24.8	26.3	.943
9b	.122	.120	2.37	1.52	11.85	5.0	1.01	19.48	.642	1.93	46.3	29.9	26.4	27.2	.971
9c	.122	.121	2.37	1.52	11.87	5.0	1.01	19.46	.643	1.93	46.2	30.0	25.6	26.9	.952
10a	.125	.123	2.37	1.76	14.17	6.0	1.02	19.02	.744	1.51	51.2	24.5	21.5	23.4	.919
10b	.125	.123	2.37	1.76	14.13	6.0	1.02	19.01	.744	1.51	51.1	24.6	21.5	22.5	.956
10c	.124	.123	2.37	1.76	14.25	6.0	1.01	19.04	.743	1.52	51.1	24.6	20.8	22.6	.920
11a	.124	.125	2.37	1.93	14.73	6.3	.99	18.98	.821	1.33	54.4	21.7	18.8	22.2	.847
11b	.124	.125	2.37	1.93	14.73	6.3	.99	18.96	.821	1.32	54.5	21.6	19.2	22.4	.857
11c	.125	.126	2.37	1.94	14.73	6.3	.99	18.89	.823	1.32	54.4	21.7	19.0	22.2	.856
12a	.120	.122	3.00	1.34	11.99	4.0	.99	25.08	.445	3.43	44.7	32.0	26.2	28.1	.932
12b	.120	.122	3.00	1.35	9.32	3.1	.99	25.03	.449	3.44	44.6	32.3	25.3	28.0	.904
13a	.120	.122	3.00	1.65	13.58	4.5	.98	25.05	.548	2.59	51.4	24.3	20.4	23.6	.864
13b	.120	.122	3.00	1.64	11.88	4.0	.98	25.03	.546	2.61	51.2	24.5	21.7	24.4	.889
13c	.120	.122	3.00	1.66	14.62	4.9	.98	25.00	.552	2.57	51.5	24.2	21.6	24.1	.896
14a	.120	.123	3.00	2.08	15.24	5.1	.98	25.00	.693	1.77	62.1	16.7	14.8	21.1	.701
14b	.120	.123	3.00	2.08	13.53	4.5	.98	24.95	.693	1.77	62.0	16.7	13.8	21.4	.646
14c	.121	.123	3.00	2.08	16.72	5.6	.98	24.90	.692	1.77	61.9	16.8	16.9	21.6	.782
15a	.120	.123	3.00	2.43	18.54	6.2	.98	25.01	.810	1.37	70.7	12.8	11.0	19.9	.553
15b	.120	.123	3.00	2.43	17.69	5.9	.98	25.01	.810	1.37	70.7	12.8	11.5	19.6	.587
15c	.120	.123	3.00	2.43	15.92	5.3	.98	24.96	.809	1.38	70.3	13.0	12.0	20.4	.588

[a] $\frac{\sigma_{cr}}{\eta} = \frac{k_W \pi^2 E_c t_W^2}{12(1-\mu^2) b_W^2}$, where E_c = 6500 ksi and μ = 0.3.

NATIONAL ADVISORY
COMMITTEE FOR AERONAUTICS

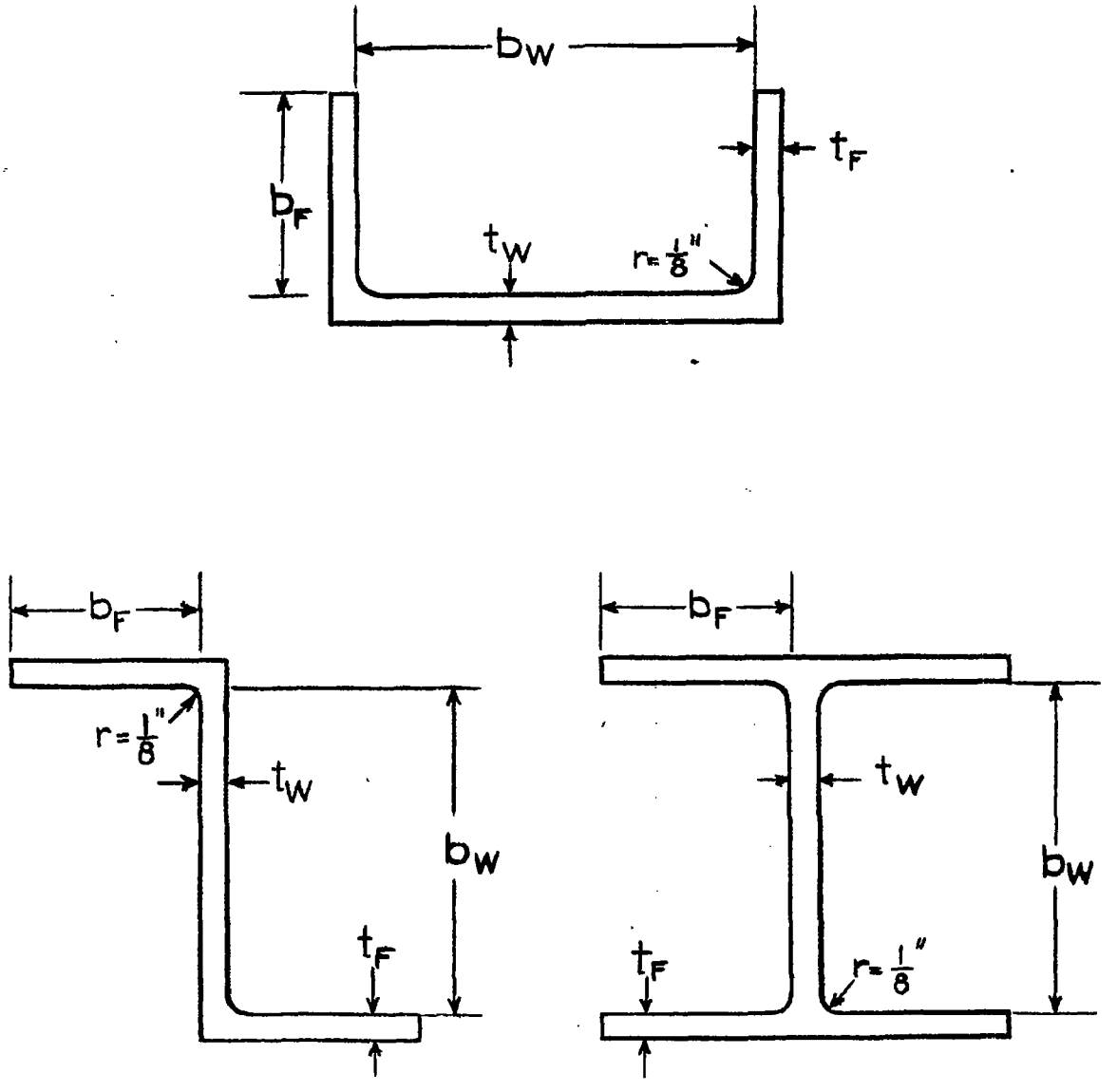

NATIONAL ADVISORY
COMMITTEE FOR AERONAUTICS

Figure 1.- Cross sections of H-, Z-, and channel-section columns.

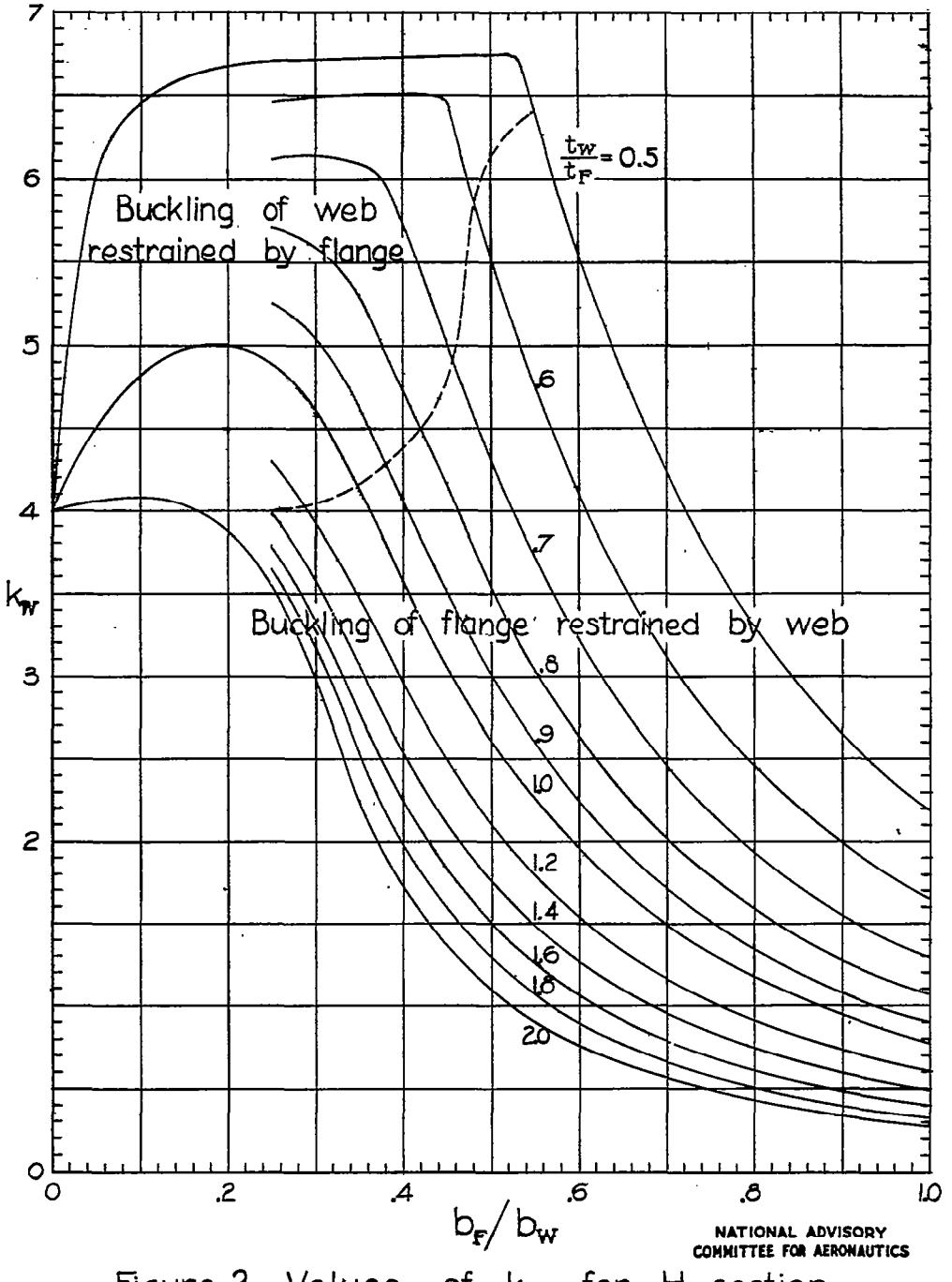

Figure 2.- Values of k_W for H-section columns. (From reference 7.)

$$\frac{\sigma_{cr}}{\eta} = \frac{k_W \pi^2 E_c t_W^2}{12(1-\mu^2) b_W^2}$$

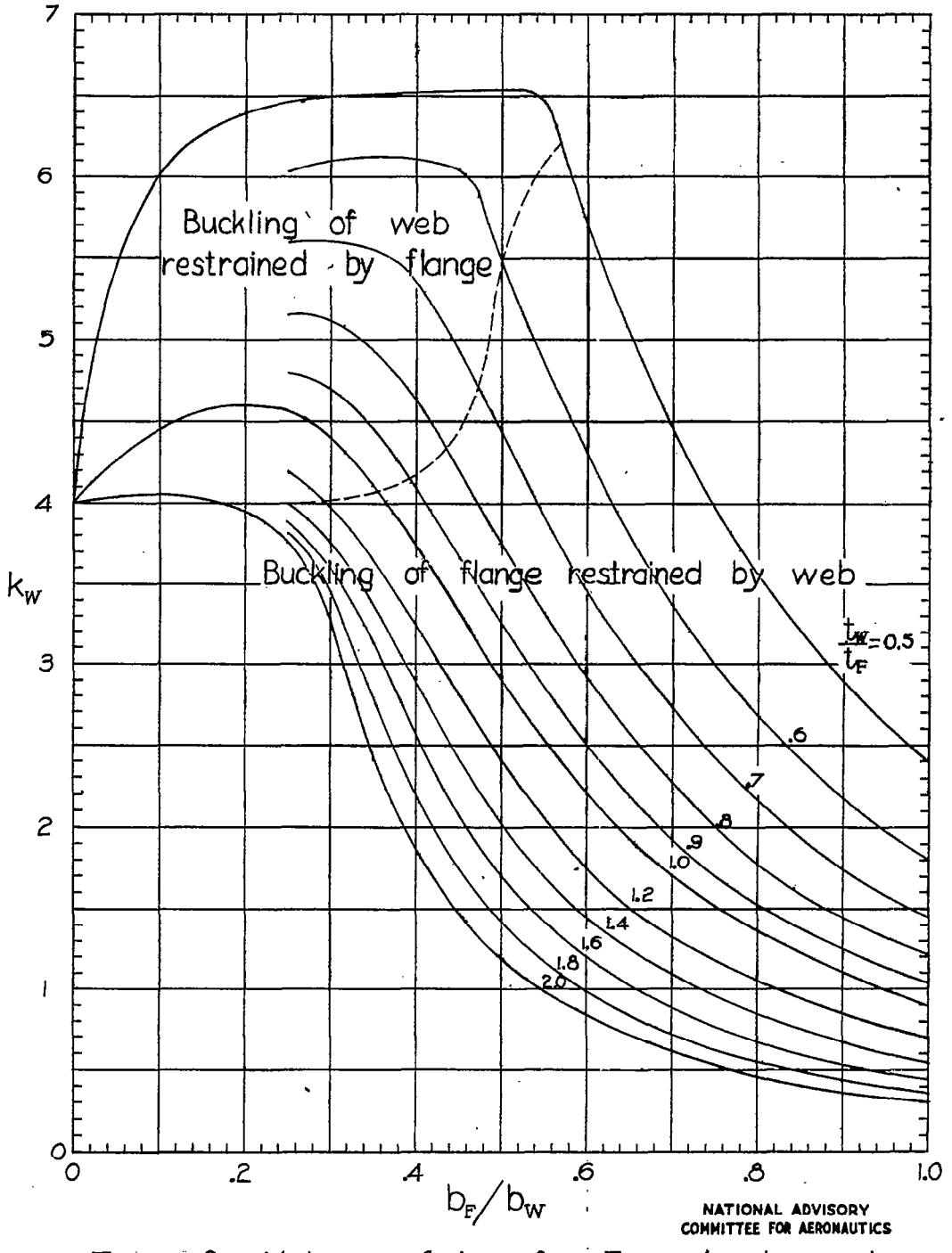

Figure 3.- Values of k_W for Z- and channel-section columns. (From reference 7.)

$$\frac{\sigma_{cr}}{\eta} = \frac{k_W \pi^2 E_c t_W^2}{12(1-\mu^2) b_W^2}$$

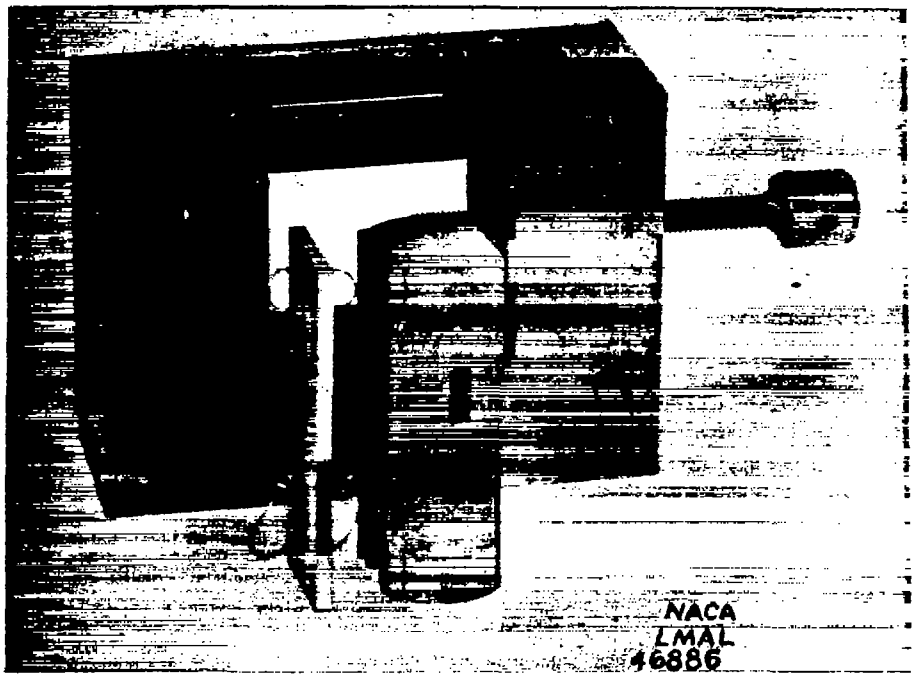

(a) Unassembled.

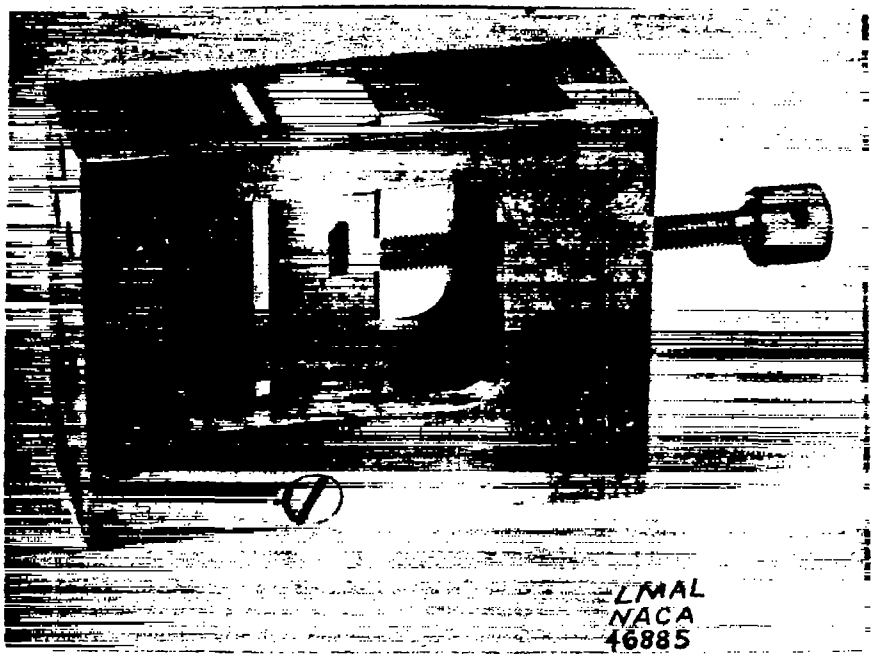

(b) Assembled.

Figure 4.- Modified Montgomery-Templin type of compression fixture using grooved steel supporting plates.

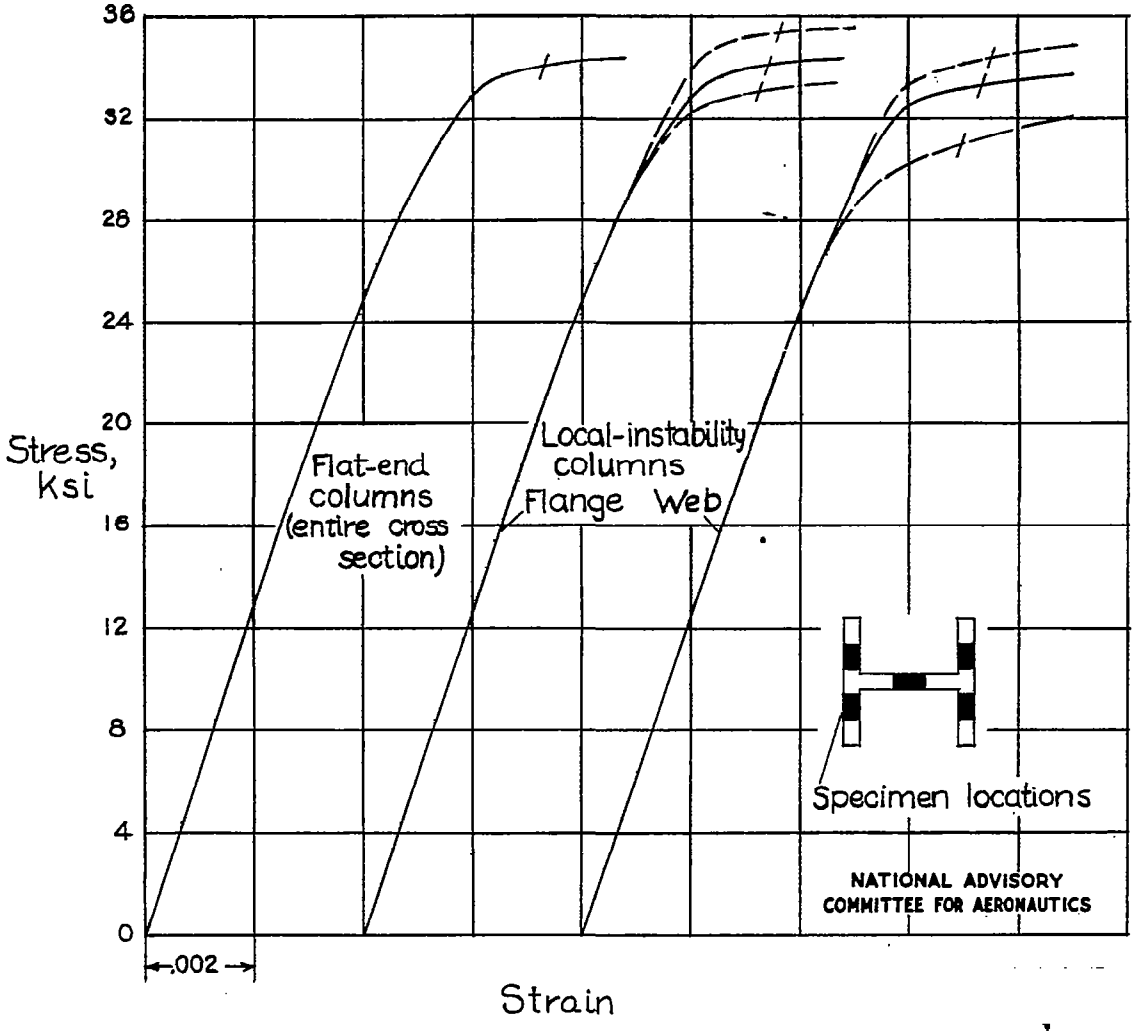

Figure 5.– Compressive stress-strain curves for extruded 0-1HTA magnesium alloy for with-grain direction.

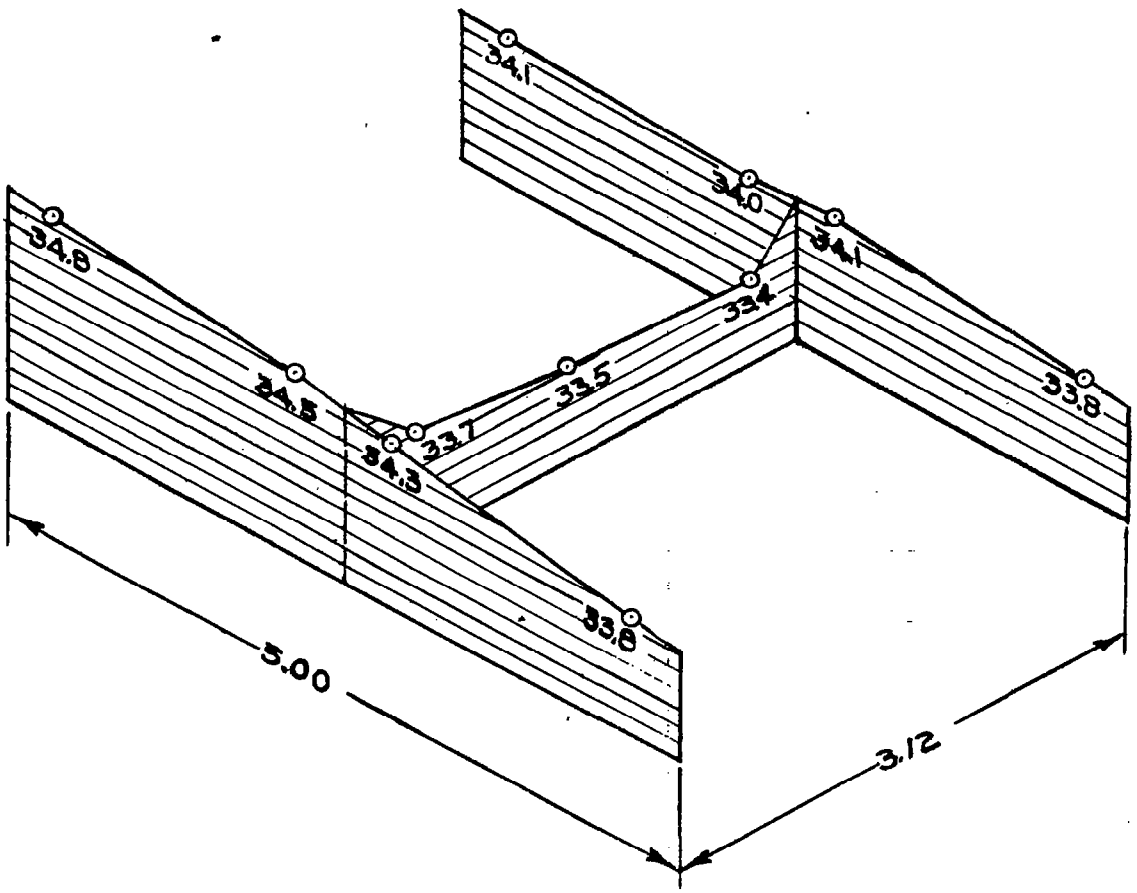

NATIONAL ADVISORY
COMMITTEE FOR AERONAUTICS

Figure 6.- Variation of compressive yield stress over a cross section of an extruded O-1HTA magnesium alloy H-section with web and flanges 0.125 inch thick. (Stress in ksi.)

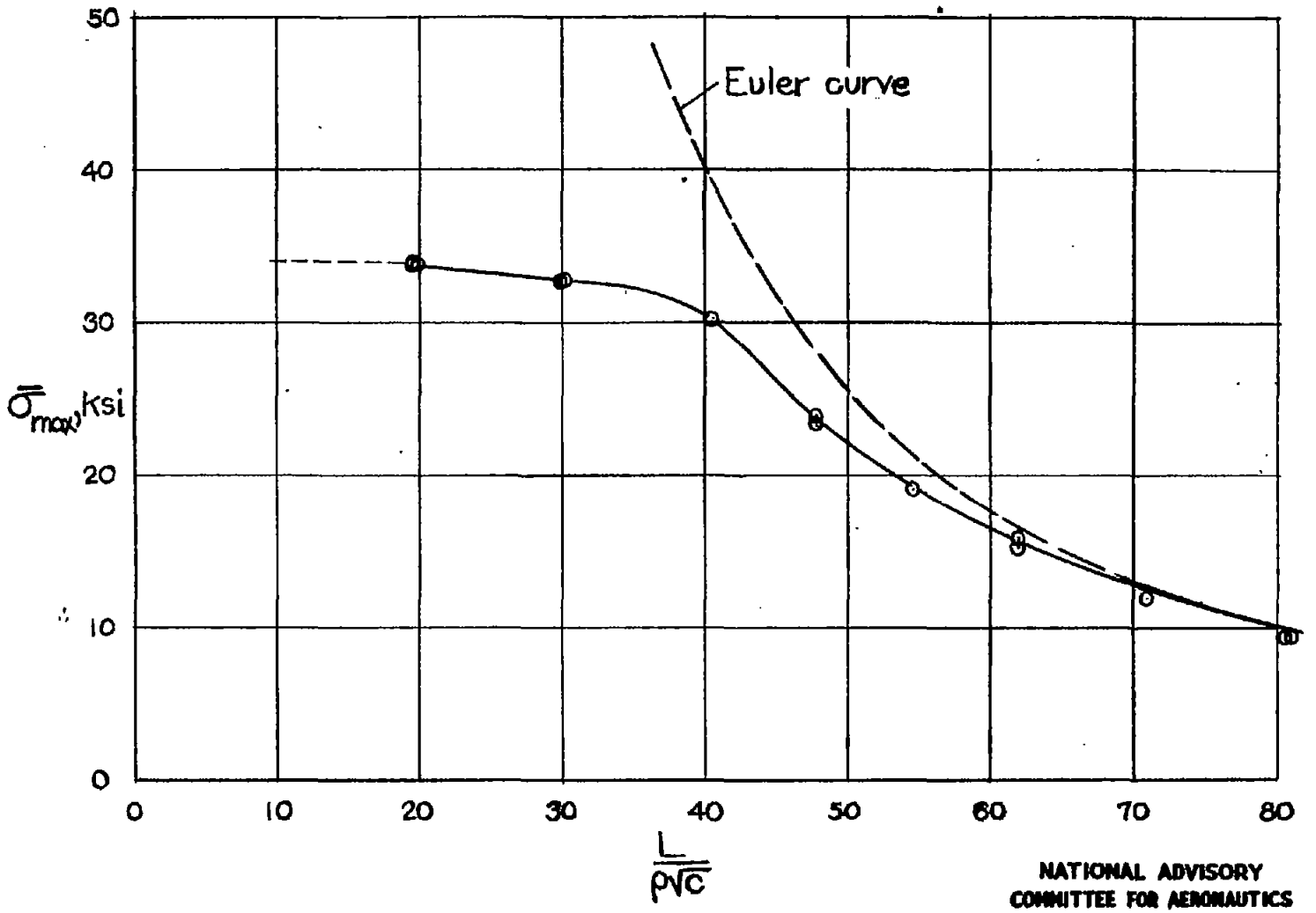

Figure 7.- Column curve for extruded O-1HTA magnesium alloy obtained from tests of flat-end H-section columns. σ_{cy}, 34 Ksi.

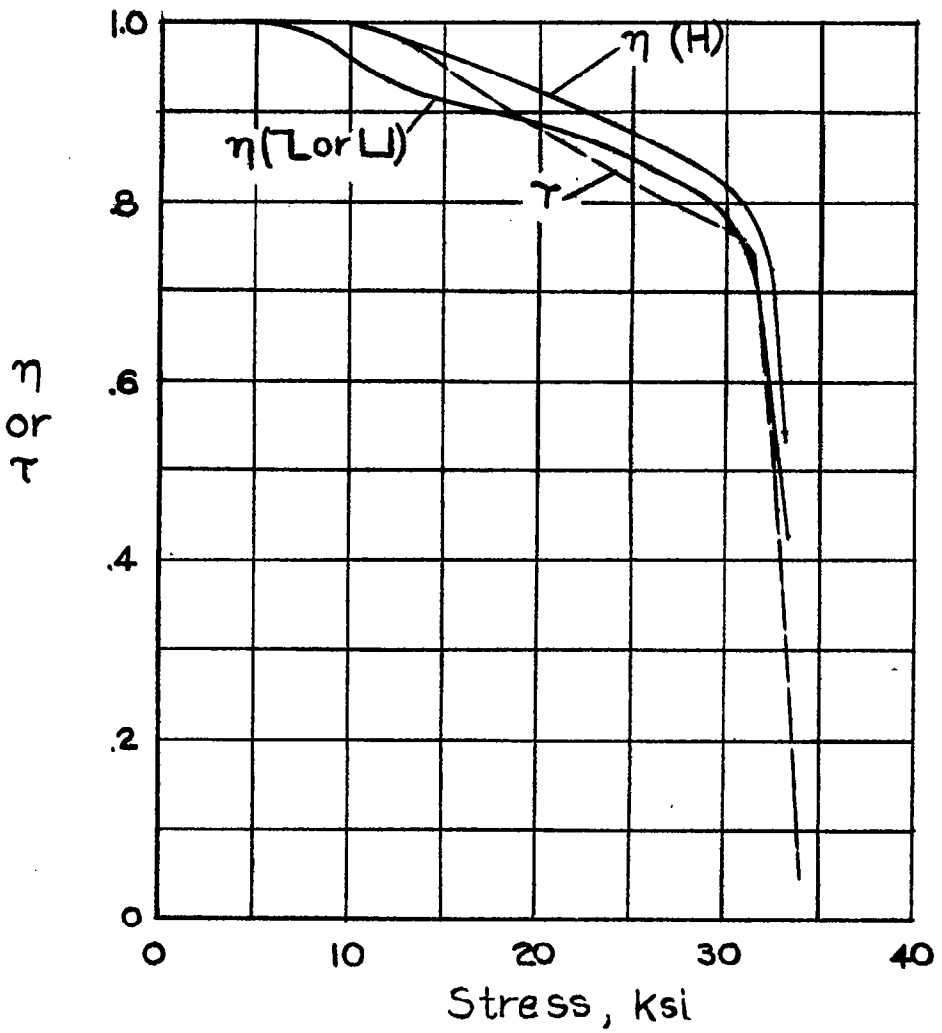

NATIONAL ADVISORY
COMMITTEE FOR AERONAUTICS

Figure 8.- Variation of τ and η with stress for extruded O-1HTA magnesium alloy. For the curve of τ; σ_{cy} (entire cross section), 34 ksi. For the curves of η, σ_{cy} (flange), 34 ksi; σ_{cy} (web), 33 ksi.

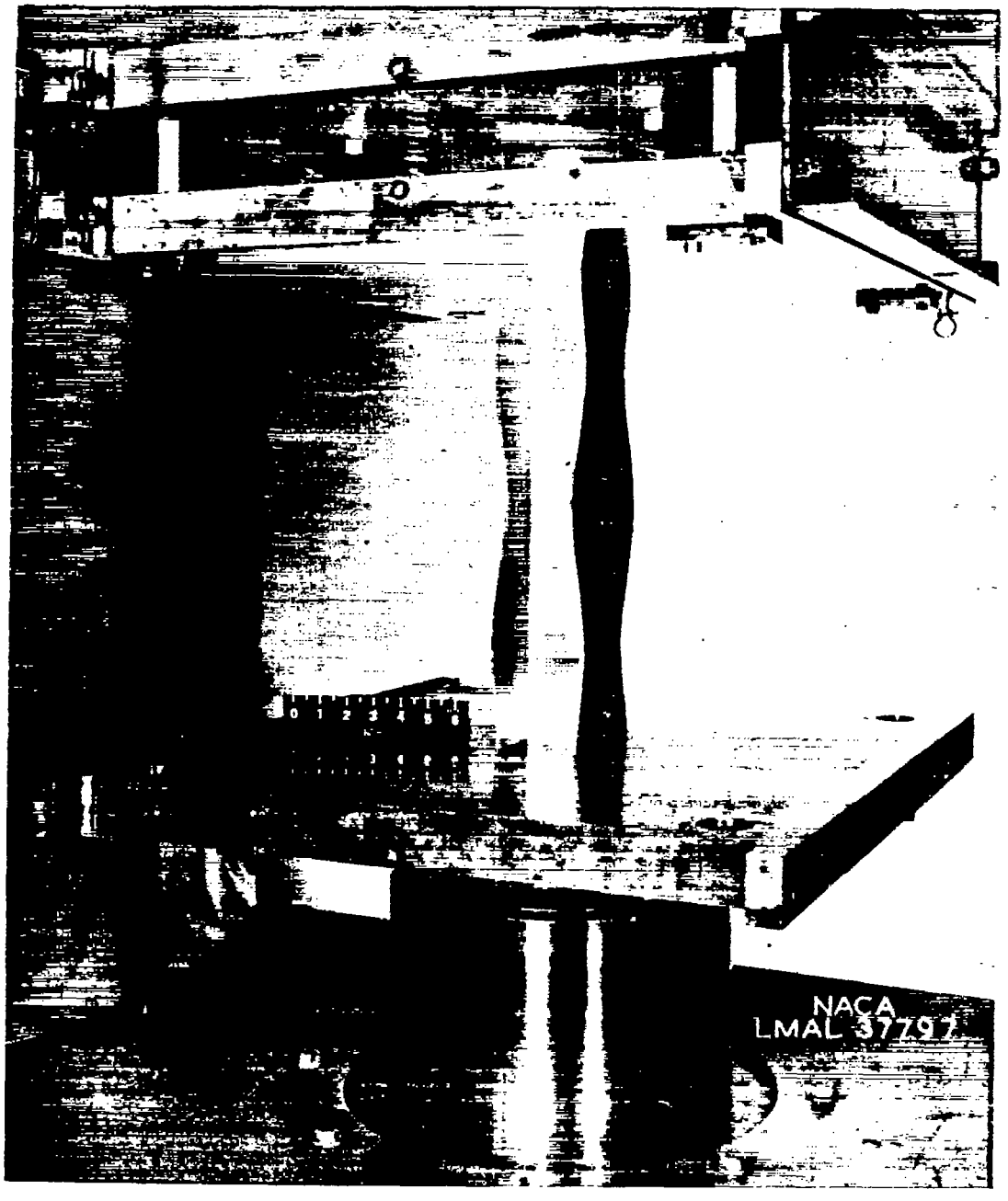

Figure 9.- Local instability of an H-section column under test.

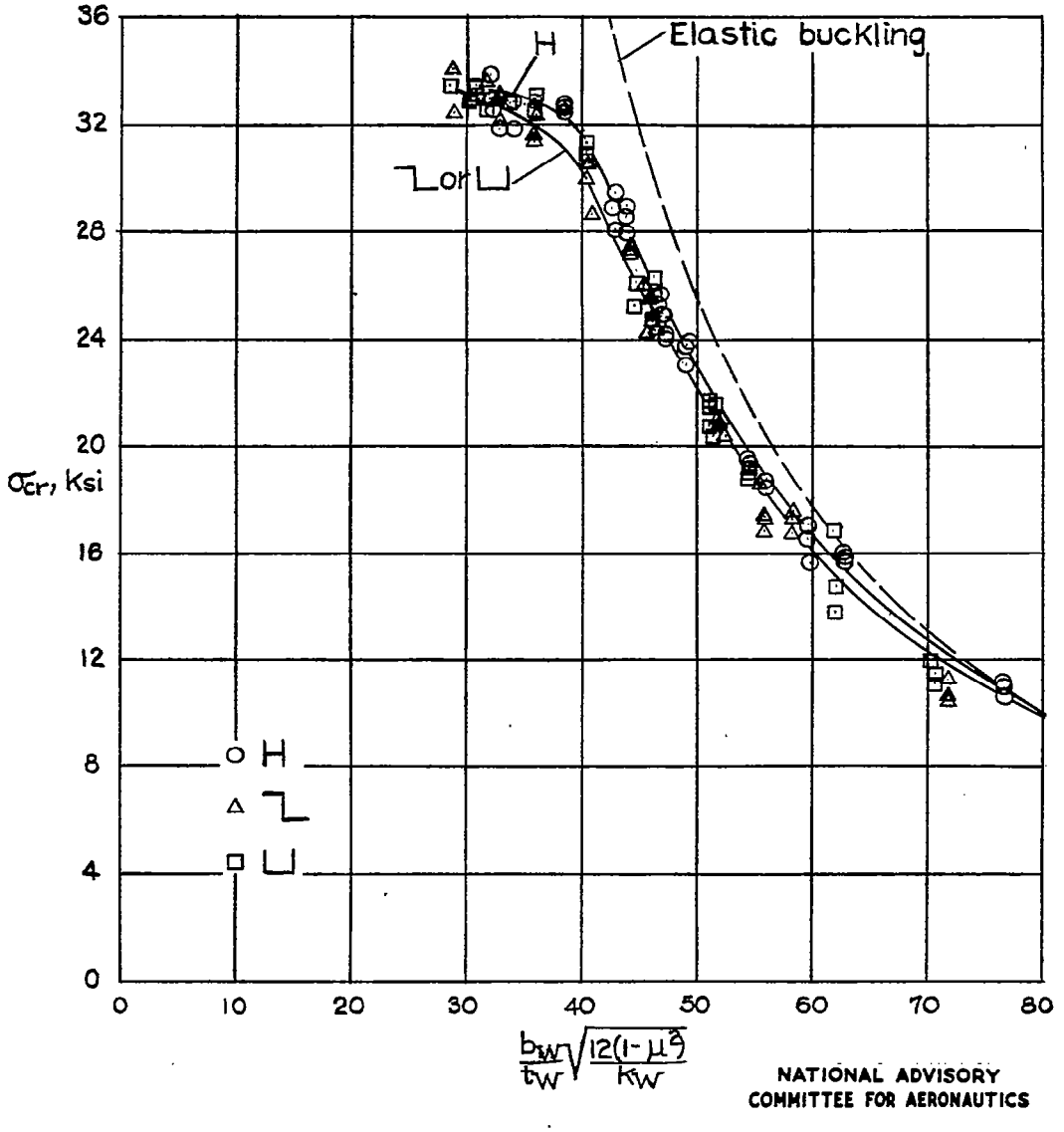

Figure 10.- Plate-buckling curves for extruded 0-1HTA magnesium alloy obtained from tests of H-, Z-, and channel-section columns. σ_{cy} (flange), 34 Ksi; σ_{cy} (web), 33 Ksi.

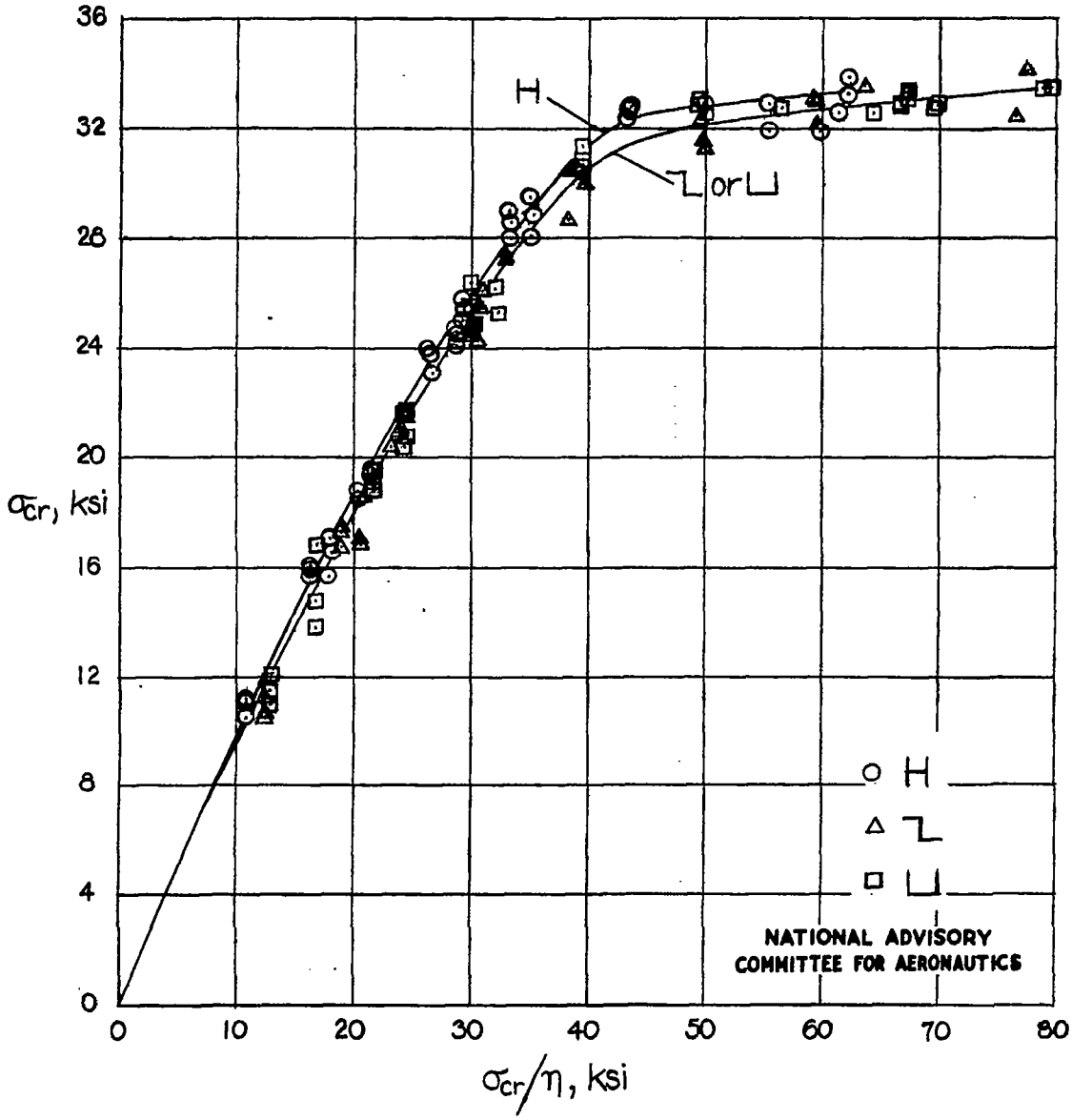

Figure 11.- Variation of σ_{cr} with σ_{cr}/η for plates of extruded O-1HTA magnesium alloy obtained from tests of H-, Z-, and channel-section columns. σ_{cy} (flange), 34 ksi; σ_{cy} (web), 33 ksi.

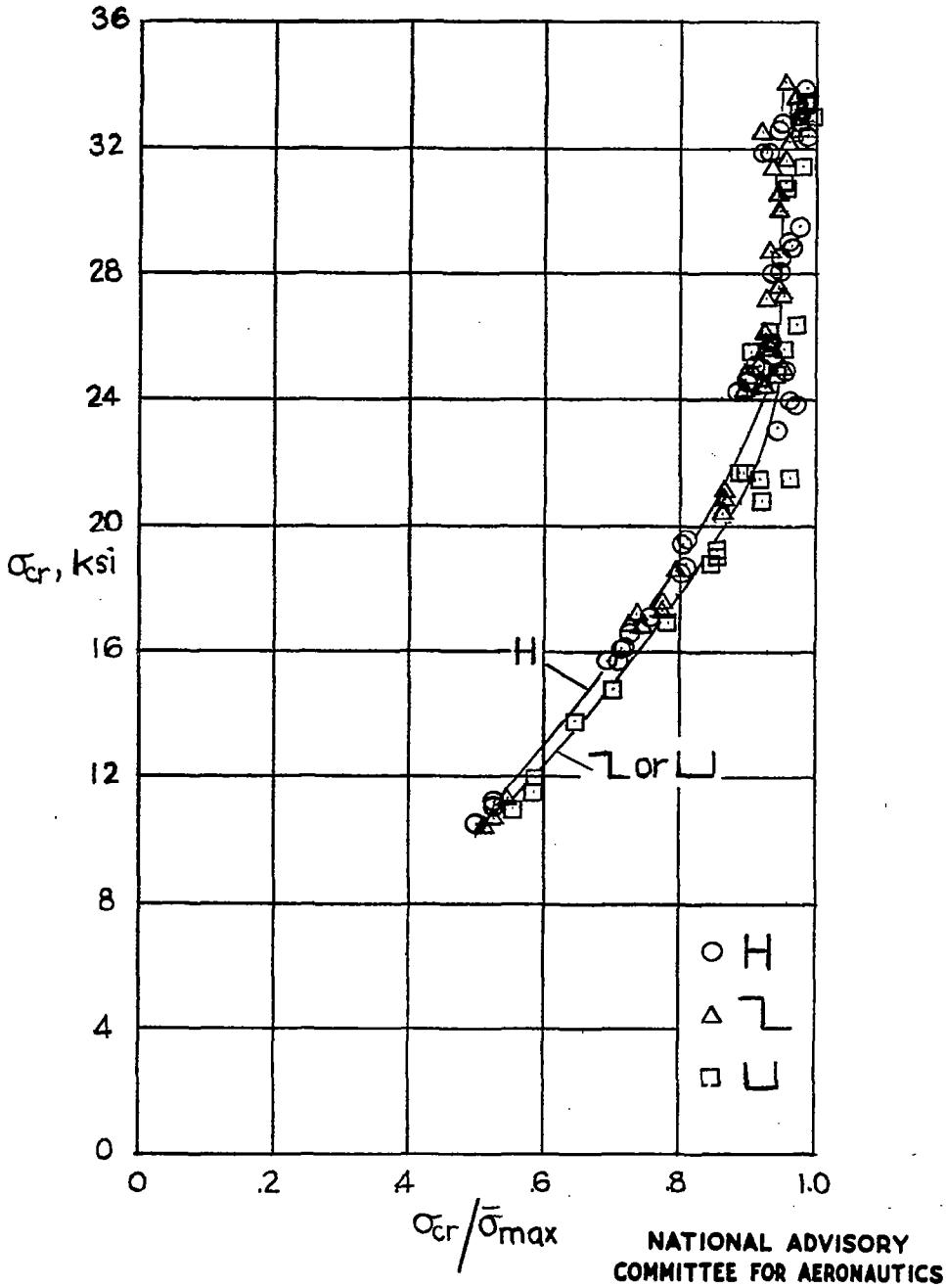

Figure 12.– Variation of σ_{cr} with $\sigma_{cr}/\bar{\sigma}_{max}$ for plates of extruded 0-1HTA magnesium alloy obtained from tests of H-, Z-, and channel-section columns. σ_{cy}(flange), 34 Ksi; σ_{cy}(web), 33 Ksi.

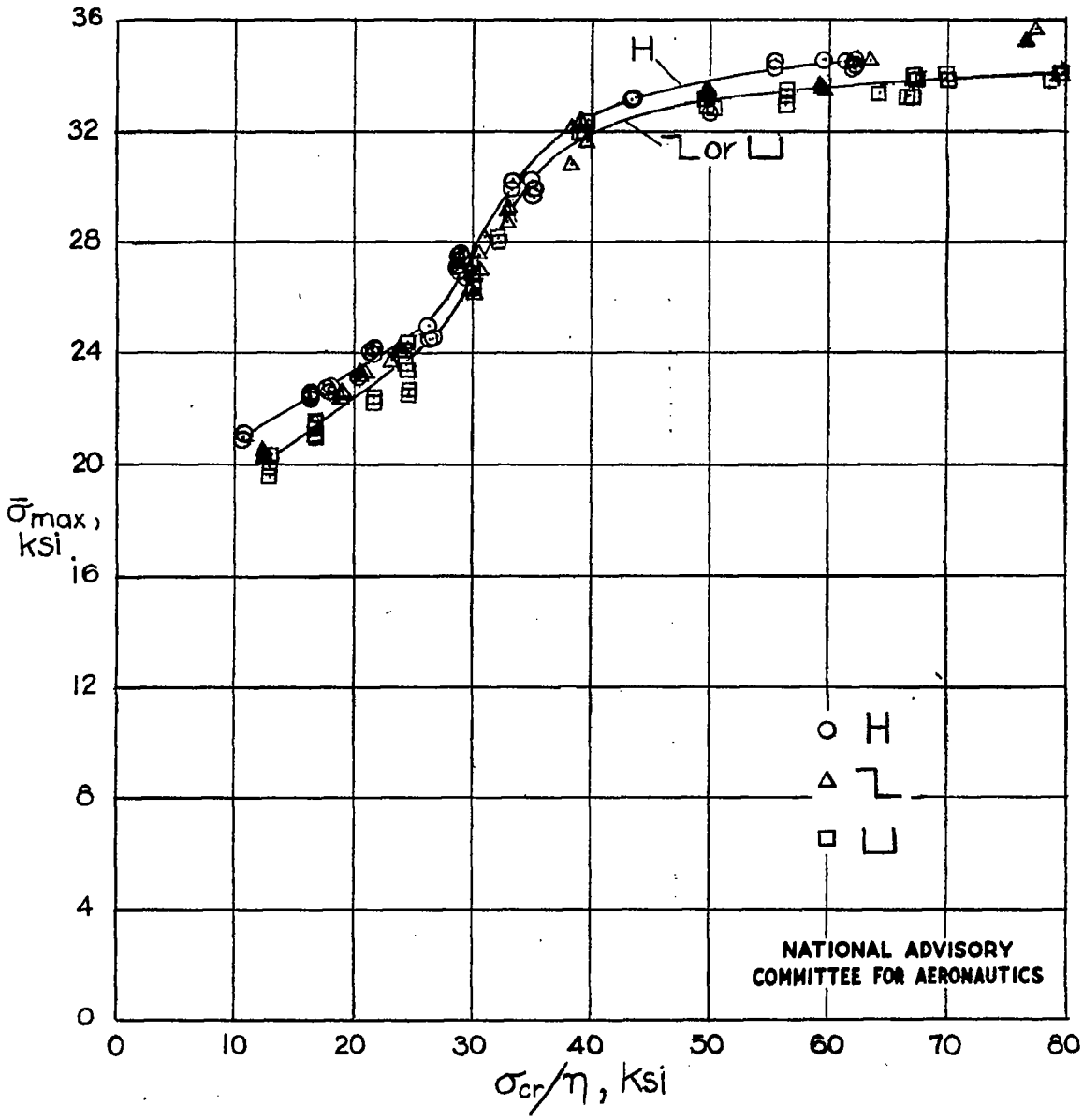

Figure 13.- Variation of $\bar{\sigma}_{max}$ with σ_{cr}/η for plates of extruded O-1HTA magnesium alloy from tests of H-, Z-, and channel-section columns. σ_{cy}(flange), 34 Ksi; σ_{cy}(web), 33 Ksi.